Corrosion Science 83 (2014) 299–309

Contents lists available at ScienceDirect

Corrosion Science

journal homepage: www.elsevier.com/locate/corsci

The cathodic behaviour of Al–Mn precipitates during atmospheric and saline aqueous corrosion of a sand-cast AM50 alloy

Mohsen Danaie [a,*], Robert Matthew Asmussen [b], Pellumb Jakupi [b], David W. Shoesmith [b], Gianluigi A. Botton [a]

[a] Department of Materials Science and Engineering, Brockhouse Institute for Materials Research and Canadian Centre for Electron Microscopy, McMaster University, Hamilton, Ontario, Canada
[b] Department of Chemistry and Surface Science Western, Western University, London, Ontario, Canada

ARTICLE INFO

Article history:
Received 18 December 2013
Accepted 14 February 2014
Available online 22 February 2014

Keywords:
A. Magnesium
A. Alloy
B. TEM
B. STEM

ABSTRACT

The behaviour of Al–Mn precipitates during atmospheric and aqueous corrosion of an AM50 Mg alloy was investigated using site-specific analytical electron microscopy. After air-exposure, localized attack was observed close to Al–Mn precipitates, with the top layer of the intermetallic enriched in Al and O. During immersed corrosion, these precipitates developed protruding domes of corrosion products, with crystalline $Mg(OH)_2$ on top and an inner layer of crystalline MgO. After prolonged immersion, these precipitates showed evidence of preferential Al dissolution, ultimately developing a fragmented interlayer of Mn_3O_4. This phase transformation is linked to the enhanced hydrogen evolution rates adjacent to these precipitates.

1. Introduction

Magnesium alloys with high strength-to-weight ratio, good castability and machinability are desirable candidate materials for automotive and aerospace applications. The major hindrance to their wider application is their susceptibility to corrosion, especially in chloride-containing aqueous environments [1]. The porosity, poor adhesion, and a narrow pH range of stability of the corrosion product (generally $Mg(OH)_2$), combined with the high electrochemical anodic activity of pure Mg results in high corrosion rates [2]. Since Mg is so anodically reactive, its corrosion can be exacerbated when the generally α-Mg matrix contains more noble secondary phases to which it can galvanically couple. Such phases are commonly incorporated in the matrix to enhance the mechanical properties of the alloy [3–5]. The presence of impurities such as Ni, Cu, and Fe can also enhance the anodic reactivity and the influence of microgalvanic coupling upon it [5,6].

The role of alloying elements is critical in optimizing the corrosion properties of Mg alloys. Addition of Mn has long been known to enhance the corrosion resistance of cast Mg alloys by capturing the residual Fe during casting [7,8]. A secondary advantage of adding Mn is grain refinement [9–11]. In the absence of Fe, numerous intermetallic phases are possible in the Al–Mn system [12]. In the Mg-rich Mg–Al–Mn ($0 \leqslant$ Mn (wt.%) $\leqslant 3$ and $0 \leqslant$ Al (wt.%) $\leqslant 15$) system it has been demonstrated, both experimentally [13] and theoretically [14], that in the melt temperature range (700–750 °C) the equilibrium phases are β-Mn (Cubic) and Al_8Mn_5 (rhombohedral). Since their atomic radii are almost equal, Fe can replace Mn in the latter phase to form the substitutional solid solution phase, $Al_8(Mn,Fe)_5$ [9].

Electrochemical measurements have shown that the Al–Mn intermetallics are cathodic with respect to the α-Mg matrix [3,15–17] (but less so than the Fe impurities that Mn is meant to capture). The eutectic intermetallic β-$Mg_{17}Al_{12}$ phase has been shown to be also weakly cathodic with respect to the α-Mg matrix [18–22], but can form a passive layer which results in an overall improvement in corrosion resistance provided that this phase is present in a continuous and uniform network [17,19,23]. The α-Mg grains themselves will have different potentials depending on the amount of Al in solid solution, with more Al resulting in slightly more noble potentials [16,24–27]. According to Mathieu et al. [16], the corrosion potential of α-Mg increases linearly, from −1.55 V_{SCE} for pure Mg to −1.40 V_{SCE} for α-Mg containing 9 at.% Al. The lowered corrosion rates of Al-rich α-Mg grains has been linked to accumulation of Al^{3+} entities on the surface [28–30], percolation of amorphous Al_2O_3 within the $MgO/Mg(OH)_2$ corrosion layer [31], and most recently shown by the present authors [32,33], to the development of a metallic Al-rich layer at the metal/corrosion layer interface.

* Corresponding author. Tel.: +1 905 525 9140x24862; fax: +1 905 521 2773.
E-mail addresses: danaiem@mcmaster.ca (M. Danaie), gbotton@mcmaster.ca (G.A. Botton).

http://dx.doi.org/10.1016/j.corsci.2014.02.030
0010-938X/

Table 1
Composition of the AM50 magnesium alloy used for this study.

Major elements (wt.%)				Minor elements (ppm-weight)				
Al	Mn	Zn	Si	P	Cu	Fe	Ni	Cr
4.42	0.29	0.09	0.02	56	23	8	4	3

In a recently proposed mechanism, based on scanning vibrating electrode measurements, Williams et al. [34] suggested a higher population of Al–Mn precipitates left in the wake of an advancing anode as the source of cathodic activity on a corroding AZ31 surface in aqueous NaCl solution. These intermetallics were also shown to coincide with the localized damage on a corroded AZ31 surface in a salt-fog environment [17]. Despite these studies, little is known about the chemical and microstructural state of these Al–Mn phases during corrosion. Recently [32], we performed site-specific analytical electron microscopy to study the microstructure of the corroded sand-cast AM50 alloy, focusing on the role of Al distribution and its effect on local corrosion behaviour. The current study applies the same experimental methodology to the Al–Mn precipitates to further understand the sequence of events occurring during the corrosion of the AM50 alloy.

2. Experimental procedure

Sand-cast AM50 alloy specimens were provided by General Motors (Canada) in the form of cylindrical ingots. The chemical composition of this alloy is presented in Table 1, and complies with the ASTM B275 standard for this alloy [35]. A detailed description of the procedures used for surface preparation and microstructural characterization of the alloy in the pristine state has been published previously [32].

Specimens were corroded in 1.6 wt.% NaCl (reagent grade, 99% assay) solution made with high purity water (HPLC grade). The sample was immersed for two periods (18 and 96 h) and then removed from the solution, washed with anhydrous ethanol and dried. Site-specific transmission electron microscopy (TEM) specimens were then prepared using the standard *in-situ* lift-out technique in a focused ion beam (FIB-Zeiss NVision 40, equipped with an X-ray energy-dispersive spectrometer XEDS – Oxford, Inca, Silicon drift detector). FIB specimens were prepared from the Al–Mn precipitates at various stages of corrosion. A specimen was also prepared from an air-exposed sample for comparison (7 days exposure to laboratory air with relative humidity between 28% and 35%). The FIB was also used in scanning electron microscopy (SEM) mode to characterize the initial microstructure.

Microscopic characterization of the FIB specimens was performed with an FEI Titan 80–300 (scanning) transmission electron microscope, (S)TEM, equipped with a Gatan Image Filter (GIF) electron energy-loss spectrometer (EELS), and an X-ray energy-dispersive spectrometer (XEDS-Oxford, Inca, Si(Li) detector). The accelerating voltage was set at 300 kV. The energy spread of the primary electron beam, measured at the full-width-at-half-maximum of the zero-loss peak in vacuum was 0.7 eV or better. In order to minimize electron beam damage, all electron microscopy characterization was performed using a cryogenically cooled sample stage (T = 95 K). Details of the electron microscopy and

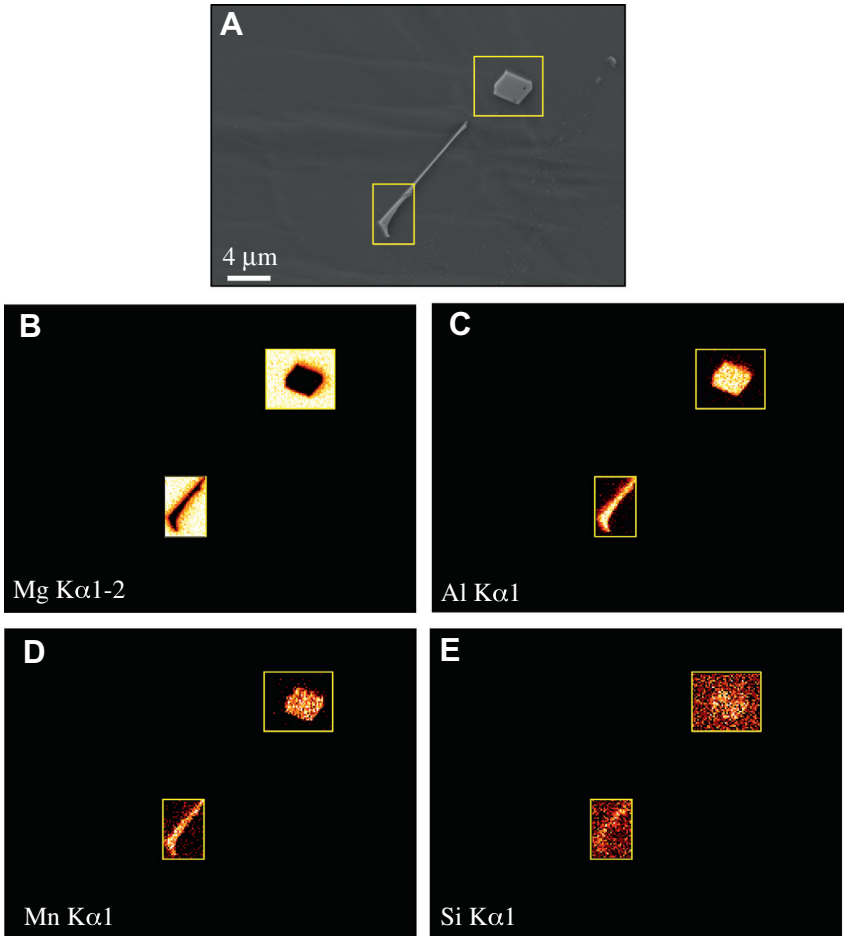

Fig. 1. (A) Area containing two edged precipitates, (B) thorough (E) XEDS elemental maps of Mg, Al, Mn, and Si of two select regions of area shown in (A).